ESC European Society of Cardiology

Cardiovascular Research (2018) **114**, 830–845
doi:10.1093/cvr/cvy030

Critical role of phosphodiesterase 2A in mouse congenital heart defects

Maria Rita Assenza[1†], Federica Barbagallo[2†], Florencia Barrios[1†], Marisa Cornacchione[3], Federica Campolo[2], Elisabetta Vivarelli[1], Daniele Gianfrilli[2], Luigi Auletta[3], Andrea Soricelli[3,4], Andrea M. Isidori[2], Andrea Lenzi[2], Manuela Pellegrini[2,5*†], and Fabio Naro[1*†]

[1]Department of Anatomical, Histological, Forensic and Orthopaedic Sciences; [2]Department of Experimental Medicine, Sapienza University of Rome, 00161 Rome, Italy; [3]IRCCS SDN, 80143 Naples, Italy; [4]Department of Motor Science and Wellness, Parthenope University, 80133 Naples, Italy; and [5]Institute of Cell Biology and Neurobiology, IBCN-CNR, 00015 Monterotondo, Rome, Italy

Received 28 July 2017; revised 4 January 2018; editorial decision 24 January 2018; accepted 1 February 2018; online publish-ahead-of-print 2 February 2018

Time for primary review: 37 days

Aims Phosphodiesterase 2 A (Pde2A), a cAMP-hydrolysing enzyme, is essential for mouse development; however, the cause of *Pde2A* knockout embryonic lethality is unknown. To understand whether Pde2A plays a role in cardiac development, hearts of *Pde2A* deficient embryos were analysed at different stage of development.

Methods and results At the stage of four chambers, *Pde2A* deficient hearts were enlarged compared to the hearts of *Pde2A* heterozygous and wild-type. *Pde2A* knockout embryos revealed cardiac defects such as absence of atrial trabeculation, interventricular septum (IVS) defects, hypertrabeculation and thinning of the myocardial wall and in rare cases they had overriding aorta and valves defects. E14.5 *Pde2A* knockouts showed reduced cardiomyocyte proliferation and increased apoptosis in the IVS and increased proliferation in the ventricular trabeculae. Analyses of E9.5 *Pde2A* knockout embryos revealed defects in cardiac progenitor and neural crest markers, increase of Islet1 positive and AP2 positive apoptotic cells. The expression of early *cTnI* and late *Mef2c* cardiomyocyte differentiation markers was strongly reduced in *Pde2A* knockout hearts. The master transcription factors of cardiac development, *Tbx*, were down-regulated in E14.5 *Pde2A* knockout hearts. Absence of Pde2A caused an increase of intracellular cAMP level, followed by an up-regulation of the inducible cAMP early repressor, *Icer* in fetal hearts. *In vitro* experiments on wild-type fetal cardiomyocytes showed that *Tbx* gene expression is down-regulated by cAMP inducers. Furthermore, Pde2A inhibition *in vivo* recapitulated the heart defects observed in *Pde2A* knockout embryos, affecting cardiac progenitor cells. Interestingly, the expression of *Pde2A* itself was dramatically affected by Pde2A inhibition, suggesting a potential autoregulatory loop.

Conclusions We demonstrated for the first time a direct relationship between Pde2A impairment and the onset of mouse congenital heart defects, highlighting a novel role for cAMP in cardiac development regulation.

Keywords CHD • Pde2A • Icer • Tbx genes

1. Introduction

Congenital heart defects (CHDs) are the most prevalent of all human birth defects (6–8 every 1000 live births)[1,2] and ventricular septum defects (VSDs) are among the most common CHDs.[2]

Unrepaired VSDs cause ventricular dilation leading to heart failure, pulmonary arterial hypertension, arrhythmias and ultimately decreased life expectancy.[3–6] The molecular causes of VSDs are mainly unknown. The most frequent genetic alterations associated to VSDs in humans and mice are mutations in transcription factors or master regulators of myocardium formation like *Nkx2.5* and *Gata4*.[7]

Hypertrabeculation and noncompaction of the myocardial wall (MW) are also common defects associated with CHDs.[8] These defects are closely tied during cardiac embryogenesis and associated to left

* Corresponding authors. Tel: +39 06 90091208; fax: +39 06 90091288, E-mail: manuela.pellegrini@cnr.it (M.P.); Tel: +39 06 49766587; fax: +39 06 4462854, E-mail: fabio.naro@uniroma1.it (F.N.)

† The first three authors and last two authors contributed equally to the study.

ventricular noncompaction (LVNC) cardiomyopathy in postnatal life.[9] The etiology and pathogenesis of this disorder are largely unknown mainly because of the lack of understanding in the underlying molecular and cellular mechanisms.

In the mouse, cardiac morphogenesis begins at E6.5-E7.5 when a subset of mesodermal cells progressively migrates antero-laterally to form the cardiac crescent.[10] At ~E8.0, the bilateral cardiac primordia coalesce and fuse at the embryonic midline to form a single primary heart tube. The primitive heart consists of two layers, an inner endocardium and the outer myocardium from which trabecular and compact zones will arise. The heart tube initiates a characteristic rightward bend, and the initial anterior–posterior polarity transforms into a right–left patterning. At E9.5, a third tissue, the epicardium, develops from splanchnic mesoderm, migrates and covers the entire myocardial surface by E11.0.[11–13] By E13.5 four chamber are formed with septa dividing atrial and ventricular chambers.[12–14]

Members of the large family of T-box (Tbx) transcription factors play a crucial role during cardiac regionalization. In the developing mammalian heart, 6 of the 17 family members of *Tbx* genes (*Tbx1, Tbx18* and *Tbx20* of the *Tbx1* subfamily and *Tbx2*, *Tbx3* and *Tbx5* of the *Tbx2* subfamily) are expressed in a combinatorial fashion in different progenitor pools and in different compartments.[15,16] Several *Tbx* mutations are associated with CHDs. For example, *TBX1* and *TBX5* loss of function mutations are, respectively, linked to the Di George and Holt-Oram syndromes in humans.[17,18]

Among the cAMP hydrolyzing phosphodiesterases (Pdes), Pde2A is essential for mouse development. In previous work, no *Pde2A* knockout newborns were found alive,[19,20] indicating that its function cannot be substituted by other Pdes. The *Pde2A* gene encodes several splice forms that are translated in five variants (NM_001143848.2, NM_001008548.4, NM_001143849.2, 001243757.1, NM_001243758.1) which contribute to differential modulation and localization of cAMP signals.[21] Pde2A activity leads to changes in cAMP/PKA-dependent gene expression through three nuclear activators: cAMP response element-binding protein (CREB), cAMP responsive element modulator (CREM) and activating transcription factor 1 (ATF-1).[22] Inducible cAMP early repressors (ICER) are members of the CREM family, which are generated through an alternative promoter in the *CREM* gene, following a cAMP surge. ICERs function inhibiting gene transcription driven by the cognates CREB and ATF-1.[23]

In this paper, we investigated whether Pde2A plays a role during heart development. The results show that hemizygous deletion of *Pde2A* gene is tolerated during embryonic and postnatal life, and the heart appears to develop normally, whereas homozygous deletion of *Pde2A* leads to fetal death before E16 and hearts show atrial defects, incomplete formation of the interventricular septum (IVS) and an alteration of the myocardium maturation. These findings were confirmed by pharmacological inhibition of Pde2A activity *in vivo*. Cell proliferation, cell survival and the electrical conduction system are altered in *Pde2A* knockout hearts. Pharmacological inhibition of Pde2A activity *in vivo* produced similar results.

Expression of cardiac progenitor and neural crest markers, as well as cardiomyocyte differentiation markers are down-regulated in both embryonic and fetal *Pde2A* knockout hearts, whereas *Tbx* genes are down-regulated and *Icer* up-regulated only in *Pde2A* deficient fetal hearts. These results correlate with an increase in intracellular cAMP levels in *Pde2A* knockout hearts. Our data indicate that Pde2A is indispensable for the early phase of heart development controlling cardiac progenitor cell and neural crest deployment and suggest that increases in cAMP play a major role in the molecular mechanism involved in the fetal heart phenotype of *Pde2A* knockout mice.

2. Methods

Detailed Methods are available in the Supplementary material online.

2.1 Mouse husbandry and *in vivo* treatments

Pde2A$^{+/-}$ mice (B6; 129P2-Pde2A < tm1Dgen>/H; EM: 02366) were obtained from EMMA (UK). Timed mating was set up between *Pde2A*$^{+/-}$ females and *Pde2A*$^{+/-}$ males or *Pde2A*$^{+/+}$ C57BL/6 male mice. Hearts of the resulting E9.5–E18.5 embryos were isolated in Hanks balanced solution (Euroclone, Italy) and processed for following analyses.

For *in vivo* treatments pregnant C57BL/6 females of 8 weeks of age were intraperitoneally injected at E4.5 or E10.5 of gestation with 0.3 mg/kg of erythro-9-(2-hydroxy-3-nonly) adenine (EHNA; Calbiochem-Merck, Germany) every 3 days until E10.5 or E13.5. Embryos were collected at E14.5. All our experimental procedures were conforming with the Directive 2010/63/EU of the European Parliament on the protection of animals used for scientific purposes and were conducted with the approval of the Sapienza University's Animal Use for Research Ethic Committee and by the Italian Ministry of Health with protocol number DGSAF 24675-A (2013).

2.2 Histology, TUNEL and immunofluorescence

Embryos at E9.5 or embryonic hearts from E11.5 and E14.5 were fixed in 4% v/v paraformaldehyde overnight at 4°C and embedded in paraffin following standard procedures. Serial sagittal or coronal sections of whole embryos (5 μm) and hearts (6 μm), respectively, were obtained and stained with hematoxylin and eosin and with Masson's Trichrome Stain Kit (Sigma-Aldrich, MO, USA) or processed for immunofluorescence After dewaxing with toluene, antigen retrieval of the sections was performed by microwave heating in 10 mM sodium citrate buffer 3 times for 5 min prior to further analyses. TUNEL staining was performed on paraffin sections using an *In situ* Cell Death Detection Kit, POD (Roche, Germany) as described in the Supplementary material online. All histological analyses were performed in a blinded way in two independent laboratories.

2.3 cAMP assay

cAMP assay was performed according to manufacturer's instructions of cAMP-Glo Assay (Promega, USA).

2.4 Cardiomyocyte culture and contraction rate

Cardiomyocytes from fetal hearts were isolated and cultured as previously reported.[20] Evaluation of beat frequency (contraction rate) was recorded as previously described.[24]

2.5 qRT–PCR

Quantitative RT–PCR was carried out as described in the Supplementary material online.

Table 1 Observed and expected genotypes of mice at different age of development

		Pde2A$^{+/+}$ (%)	*Pde2A*$^{+/-}$(%)	*Pde2A*$^{-/-}$ (%)	Adsorbed (%)	Total N
E 9.5	Observed	32.5	53.5	14.0	—	43
	Expected	25.0	50.0	25.0		
E 11.5–13.5	Observed	30.4	48.7	20.9	0.008	115
	Expected	25.0	50.0	25.0		
E 14.5–15.5	Observed	28.0	43.6	28.4	0.040	303
	Expected	25.0	50.0	25.0		
1–2 dpp	Observed	37.0	63.0	0.80	—	119
	Expected	25.0	50.0	25.0		

2.6 Statistical analyses

All data are expressed as mean ± SEM and analysed with one-way or two-way analysis of variance (ANOVA) with Bonferroni correction (Bonferroni post hoc Test), Student's *t*-test or Fisher's exact test. Differences were considered significant if $^{*}P < 0.05$.

3. Results

3.1 Pde2A deficient embryos display morphological defects associated with heart malformations

We did not find any *Pde2A*$^{-/-}$ embryos alive after 15.5 day of gestation onwards except for one pup that was born dead (see *Table 1*) confirming that *Pde2A* knockout mice die in utero.[19,20] From E13.5, it was possible to recognize *Pde2A*$^{-/-}$ embryos because of their small size, pale appearance, small liver and diffuse hemorrhages (*Figure 1A*). Many *Pde2A*$^{-/-}$ embryos displayed nuchal edema under the skin on the front of the head and in the occipital region (*Figure 1A*). Since nuchal edema is frequently associated with CHDs,[25] the presence of cardiac alterations was investigated in isolated hearts from *Pde2A*$^{-/-}$ embryos.

At E11.5, no gross morphological differences were observed in the formation of the heart tube of *Pde2A*$^{+/-}$ or *Pde2A*$^{-/-}$ mice (see Supplementary material online, *Figure S1A and B*). At E14.5, the heart weight was slightly increased in *Pde2A*$^{-/-}$ (3.37 ± 0.38 mg) embryos compared to hearts of *Pde2A*$^{+/-}$ (3.08 ± 0.25 mg) and *Pde2A*$^{+/+}$ (2.53 ± 0.40 mg) embryos. Moreover, *Pde2A* knockout hearts were enlarged and the basal side of the ventricular surcus appeared wider compared to the heterozygous and wild-type (*Figure 1B* and *C*). Quantitative assessment of ventricular proximo–distal and contralateral axes evidenced that the observed enlargement is mainly due to an increase of the contralateral axis in the knockouts (*Pde2A*$^{+/+}$ 1.63 ± 0.04 mm, *Pde2A*$^{+/-}$ 1.7 ± 0.08 mm vs. *Pde2A*$^{-/-}$ 1.99 ± 0.10 mm in hematoxylin and eosin stained sections, *Figure 1D*). No differences were observed in the length of the proximo-distal axis (*Figure 1E*). These data suggest that *Pde2A* gene deletion affects the heart size and leads to ventricular dilatation.

3.2 Pde2A deficiency is associated with IVS defects and thin MW

Microscopic examination revealed that knockout but not heterozygous heart sections have defective atria with smooth walls compared to the trabeculated atria walls of wild-type embryos (*Figure 1C* and Supplementary material online, *S1C*). Moreover, a subset of mice showed atrial septal defects (see Supplementary material online, *Figure S1C and Table 2*). The IVS of *Pde2A*$^{-/-}$ hearts at E13.5–14.5 had a normal width (*Figure 1F*), but it was not completely formed preventing the separation of the right and the left ventricles (*Figure 1C* and Supplementary material online, *Figure S2A, C*). IVS were normally formed in *Pde2A* heterozygous littermates (see Supplementary material online, *Figure S1C*).

The MW of *Pde2A*$^{-/-}$ hearts was ∼ 65% thinner compared to the wall of *Pde2A*$^{+/+}$ and *Pde2A*$^{+/-}$ hearts (*Pde2A*$^{-/-}$ 41.75 ± 4.4 μm vs. *Pde2A*$^{+/-}$ 110 ± 9.3 μm and *Pde2A*$^{+/+}$ 125 ± 6.1 μm; *Figure 1C, G* and *Table 2*). *Pde2A*$^{-/-}$ also displayed hypertrabeculation of the ventricular myocardium as evidenced by the presence of thicker trabeculae (*Pde2A*$^{-/-}$ 31.6 ± 1.47 μm vs. *Pde2A*$^{+/-}$ 28.93 ± 0.66 μm and *Pde2A*$^{+/+}$ 26.98 ± 1.08 μm; *Figure 1C, H* and *Table 2*) which were of greater number (*Pde2A*$^{-/-}$ 20.38 ± 0.89 vs. *Pde2A*$^{+/-}$ 16.32 ± 0.6 and *Pde2A*$^{+/+}$ 14.90 ± 0.89 measured in 0.2 mm^2; *Figure 1C, I* and *Table 2*). Wall and trabecular defects were similarly observed in the right and left ventricles (see Supplementary material online, *Figure S2B*). Further analyses revealed that a subset of *Pde2A*$^{-/-}$ mice showed more heart abnormalities such as overriding aorta, valves (see Supplementary material online, *Figure S2A* and *Table 2*) with rare occurrences of double-outlet right ventricles and outflow tract defects (data not shown and *Table 2*).

Enlargement of ventricles was not associated with fibrotic tissue deposition since histological analysis did not reveal any difference in the presence of fibrotic tissue, between hearts of *Pde2A*$^{+/+}$ and *Pde2A*$^{-/-}$ mice, with the composition of the extracellular matrix appearing normal both in IVS and MW (see Supplementary material online, *Figure S2C*). To explore whether these defects were associated to a modification of cAMP levels in fetal hearts, a measurement of the cyclic nucleotide was performed. As shown in *Figure 1J*, *a* significant increase in cAMP level was observed in the hearts of knockout embryos at E14.5, suggesting that Pde2A activity impairment is not recovered by other cAMP hydrolyzing Pdes.

3.3 *Pde2A*$^{-/-}$ hearts show altered cell proliferation and increased cell death

Since the septum and ventricular wall defects could be due to an increase of cell death rate or a decrease of cell proliferation in these regions, both effects were analyzed. Cell proliferation was evaluated by Ki67 staining in E14.5 heart sections. A significant reduction of cell proliferation was observed in IVS, whereas a significant increase was recorded in ventricular trabeculae (VT) of *Pde2A*$^{-/-}$ hearts compared to *Pde2A*$^{+/+}$ and *Pde2A*$^{+/-}$ (*Figure 2A* and data not shown; 44.98% ± 2.19 vs. 30.64% ± 2.16

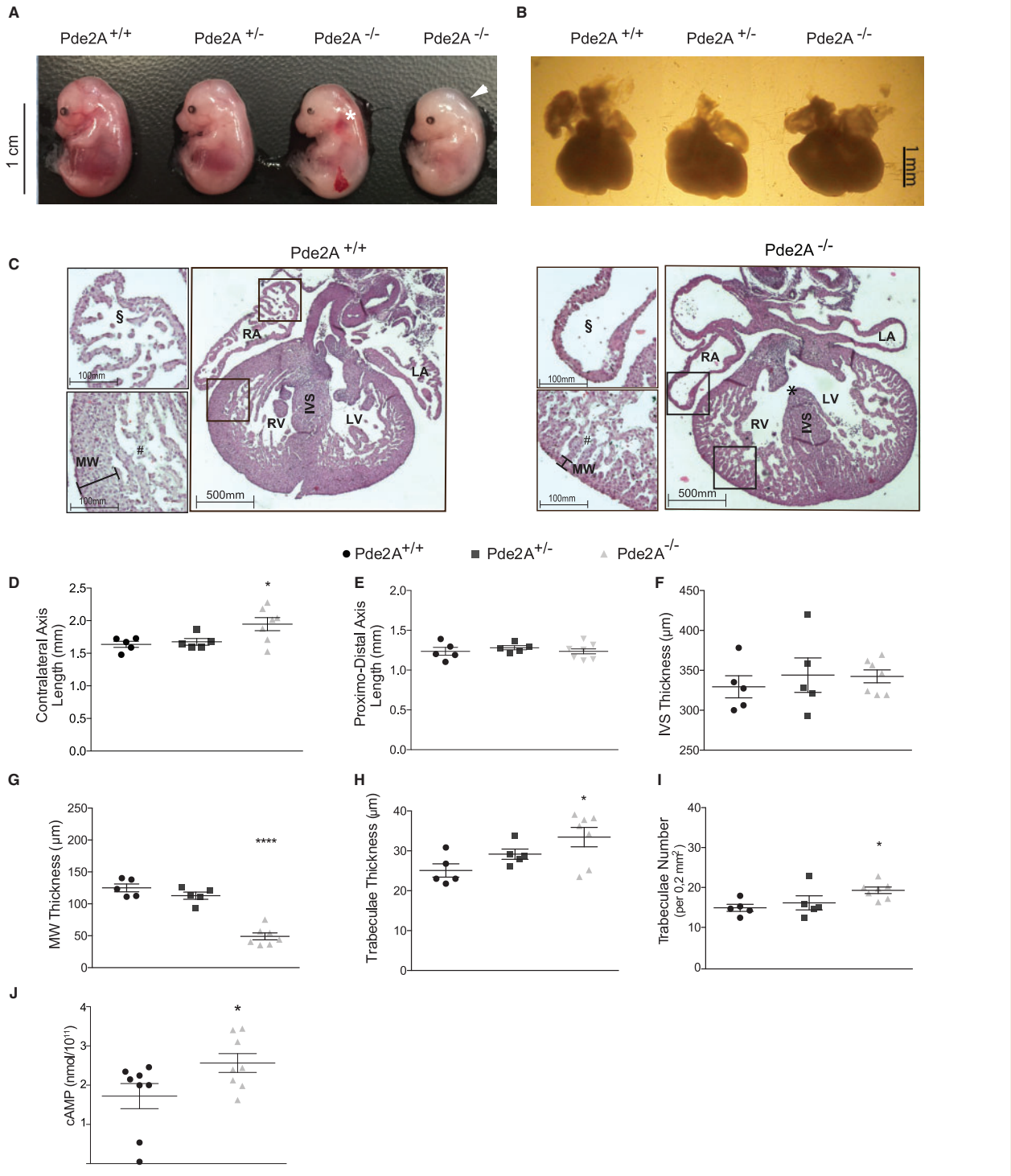

Figure 1 Pde2A deficiency is associated to congenital heart defects. (*A*) Embryos from *Pde2A*$^{+/-}$ intercrosses at E14.5. White arrow indicates nuchal edema expanding from the front of the head into the back, shows diffuse hemorrhage. (*B*) Representative images of hearts isolated from E14.5 *Pde2A*$^{+/+}$, *Pde2A*$^{+/-}$ and *Pde2A*$^{-/-}$ embryos. (*C*) Hematoxylin & Eosin staining of E14.5 hearts. * indicates incomplete formation of the IVS in *Pde2A*$^{-/-}$ hearts. Section magnifications display the myocardial compaction and atrial trabeculae: § indicates the absence of trabeculation in *Pde2A*$^{-/-}$ atria and # indicates the hyper-trabeculation in *Pde2A*$^{-/-}$ ventricles. Black bars indicate the thickness of compact myocardium (MW) in *Pde2A*$^{+/+}$ and *Pde2A*$^{-/-}$ hearts. (D-*G*) dot plots show the contralateral (*D*), and proximo-distal (*E*) axes lengths and IVS (*F*), and MW (*G*) thicknesses on *Pde2A*$^{+/+}$, *Pde2A*$^{+/-}$, *Pde2A*$^{-/-}$ sectioned hearts. Each dot represents the analysis of 30 sections/embryo. Dot plots show trabeculae thickness (*H*) and trabeculae number (*I*) in E14.5 *Pde2A*$^{+/+}$, *Pde2A*$^{+/-}$, *Pde2A*$^{-/-}$ sectioned hearts. n = 30 trabeculae/embryo (H) and n = 48 fields of 0.2 mm^2/24 sections/embryo (I) were quantified. At least five embryos were analyzed for each genotype. The mean value ± SEM is shown and one-way ANOVA with Bonferroni post hoc test was used for statistical analyses. *P<0.05, ****P<0.0001. (*J*) Quantification of cAMP level was performed in n = 8 hearts from E14.5 *Pde2A*$^{+/+}$ and *Pde2A*$^{-/-}$ embryos. The mean value ± SEM is shown and Student's t-test was used for statistical analysis. *P<0.05.

Table 2 Penetrance and Fisher's exact test of congenital heart defects observed in E14.5 *Pde2A*$^{-/-}$ embryos ($n = 7$)

	Defects (%)	Fisher's test (vs *Pde2A*$^{+/+}$)
ASD	29	0.5
Smooth atria	100	0.0006***
VSD	100	0.0006***
Ventricular hypertrabeculation	100	0.0006***
Wall noncompaction	86	0.0050**
AO	29	0.5
DORV	14	1.0
Valves defects	29	0.5
OFTD	14	1.0

ASD, atrial septal defects; VSD, ventricular septal defects; AO, overriding aorta; DORV, double outlet right ventricle; OFTD, outflow tract defect.
**$P < 0.01$.
***$P < 0.001$.

in the IVS of wild-type and knockout hearts, respectively; 12.60% ± 1.31 vs. 30.92% ± 3.55 in the VT of wild-type and knockout hearts, respectively). Further analyses revealed that cardiomyocyte proliferation was impaired and the cardiomyocyte number decreased IVS of knockout mice as revealed by staining with a pan antibody for myosin heavy chain (see Supplementary material online, *Figure S3*). Apoptotic cells were increased in the apex and in the IVS of *Pde2A*$^{-/-}$ hearts compared to *Pde2A*$^{+/+}$ and *Pde2A*$^{+/-}$ (*Figure 2B* and data not shown; 4.47% ± 0.41 vs. 7.4% ± 0.7 in the apex of wild-type and knockout hearts, respectively; 8.76% ± 1.38 vs. 18.28% ± 1.98 in the IVS of wild-type and knockout hearts, respectively). The increase in apoptosis of hearts of knockout embryos was confirmed by western blot data analyses measuring the apoptotic marker Bak and the pro-survival marker Bcl-x_L. As shown in *Figure 2C*, the expression of Bak was increased and Bcl-x_L was decreased in the hearts of *Pde2A*$^{-/-}$ embryos compared to expression in the hearts of wild-type mice.

To further uncover which particular cell lineage was affected by the deletion of *Pde2A* gene, qRT–PCR was performed on specific markers for cardiomyocytes (*Mef2c*), fibroblasts (*Vimentin*), endothelial (*CD31*) and smooth muscle (*α-SMA*) cells. A substantial reduction of *Mef2c* and *Vimentin* mRNAs was observed in *Pde2A*$^{-/-}$ hearts, whereas *CD31* and *α-SMA* markers were not affected (*Figure 2D*).

Pathological ventricular remodelling could be also due to cell growth alteration. For this reason, the area of isolated cardiomyocytes was measured to assess whether cardiomyocyte growth was increased in *Pde2A*$^{-/-}$ mice. Analysis of fetal cardiomyocytes harvested from hearts at E14.5 showed no difference in cell size between *Pde2A*$^{-/-}$ and *Pde2A*$^{+/+}$ mice (see Supplementary material online, *Figure S4*). Altogether these results indicate that the IVS and hypertrabeculation defects in *Pde2A*$^{-/-}$ mice are likely due to an imbalance between cardiomyocyte precursor proliferation and apoptosis.

3.4 *Pde2A*$^{-/-}$ cardiomyocytes show beating alteration and increased connexin 43 (Cx43) expression

Since *Pde2A* knockout hearts show increased cAMP levels and our previous results demonstrated that stimulation of Pde2A activity modulates contraction rate after beta adrenergic stimulation,[20] beating frequency of *Pde2A*$^{-/-}$ cardiomyocytes was measured.[24] As shown in *Figure 3A*, cardiomyocytes from *Pde2A* knockout mice spontaneously contract *in vitro* as the wild-types. However, the contraction rate is faster in *Pde2A* knockout cardiomyocytes and beating was blunted more frequently ($N = 3$ over 9 beating syncytia) compared to cardiomyocytes obtained from wild-type and heterozygous embryos, suggesting possible arrhythmias in *Pde2A* knockout fetal hearts. These observations encouraged us to investigate the expression and localization of Cx43, a marker of gap junctions that modulate the electrical conduction system in the heart. An increase of Cx43 expression (*Figure 3B–D*) with no evident change in localization (*Figure 3C* and *D*) was revealed in *Pde2A*$^{-/-}$ ventricles. These data indicate that Pde2A might affect cardiomyocyte contraction rate by Cx43 modulation.

3.5 The Tbx transcription factors are down-regulated and Icer is up-regulated in *Pde2A*$^{-/-}$ hearts

To understand the molecular basis of cardiac defects detected in *Pde2A* knockouts, the expression of critical genes involved in cardiac development was evaluated in hearts obtained from E14.5 *Pde2A*$^{+/+}$ and *Pde2A*$^{-/-}$ littermates (*Figure 4A*). As revealed by real time PCR, *Bmp10* gene, responsible of cardiomyocyte proliferation in trabecular myocardium,[26,27] was robustly up-regulated in samples obtained from *Pde2A*$^{-/-}$ hearts when compared to its expression in samples obtained from the heart of *Pde2A*$^{+/+}$ littermates (*Figure 4A*).

Expression of all *Tbx* genes was significantly reduced in *Pde2A*$^{-/-}$ hearts when compared to the expression levels observed in the heart of *Pde2A*$^{+/+}$ littermates (*Figure 4A*). The expression of *Fgf10*, a direct downstream target of Tbx1,[28] was also strongly down-regulated (*Figure 4A*). These results suggest that Pde2A activity is critical for the expression of *Tbx* gene families and their downstream effectors which are associated to IVS and MW development. Since Tbx families can be modulated by Bmp2/4 receptors and Notch signalling,[29,30] their expression was also investigated. Neither *Bmp* receptors nor *Notch/Hey2* gene expression was modified in *Pde2A*$^{-/-}$ hearts (see Supplementary material online, *Figure S5*).

To investigate the possible mechanism by which the absence of Pde2A can regulate Tbx expression we focused on Icer, a cAMP-dependent transcription repressor found to be up-regulated in cardiomyocytes treated with an inhibitor of the cAMP hydrolyzing phosphodiesterase 3 A (Pde3A).[31] We hypothesized that Icer expression could be also increased in embryonic hearts of *Pde2A*$^{-/-}$ as a consequence of increased intracellular cAMP level increase. qRT–PCR analyses revealed a significant up-regulation of *Icer* mRNA in *Pde2A*$^{-/-}$ hearts compared to *Pde2A*$^{+/+}$ (*Figure 4A*). In line with mRNAs levels, western blot analyses showed that the amount of Icer protein isoforms was increased in *Pde2A*$^{-/-}$ hearts (*Figure 4B*), whereas *Tbx1* and *Tbx20* expression was reduced (*Figure 4B*). These results suggest that Icer is the transcriptional repressor responsible of *Tbx* down-regulation in the hearts of E14.5 *Pde2A* knockout embryos.

3.6 *Tbx* expression is regulated by cAMP inducers and Pde2A activity

To test the hypothesis that Tbx gene expression depends on the intracellular level of cAMP, cardiomyocytes from E14.5 *Pde2A*$^{+/+}$ were isolated and cultured for 48 h in the presence of 10 µmol/L Bay 60-7550, a potent Pde2A inhibitor and/or 10 µmol/L isoproterenol (Iso), a drug

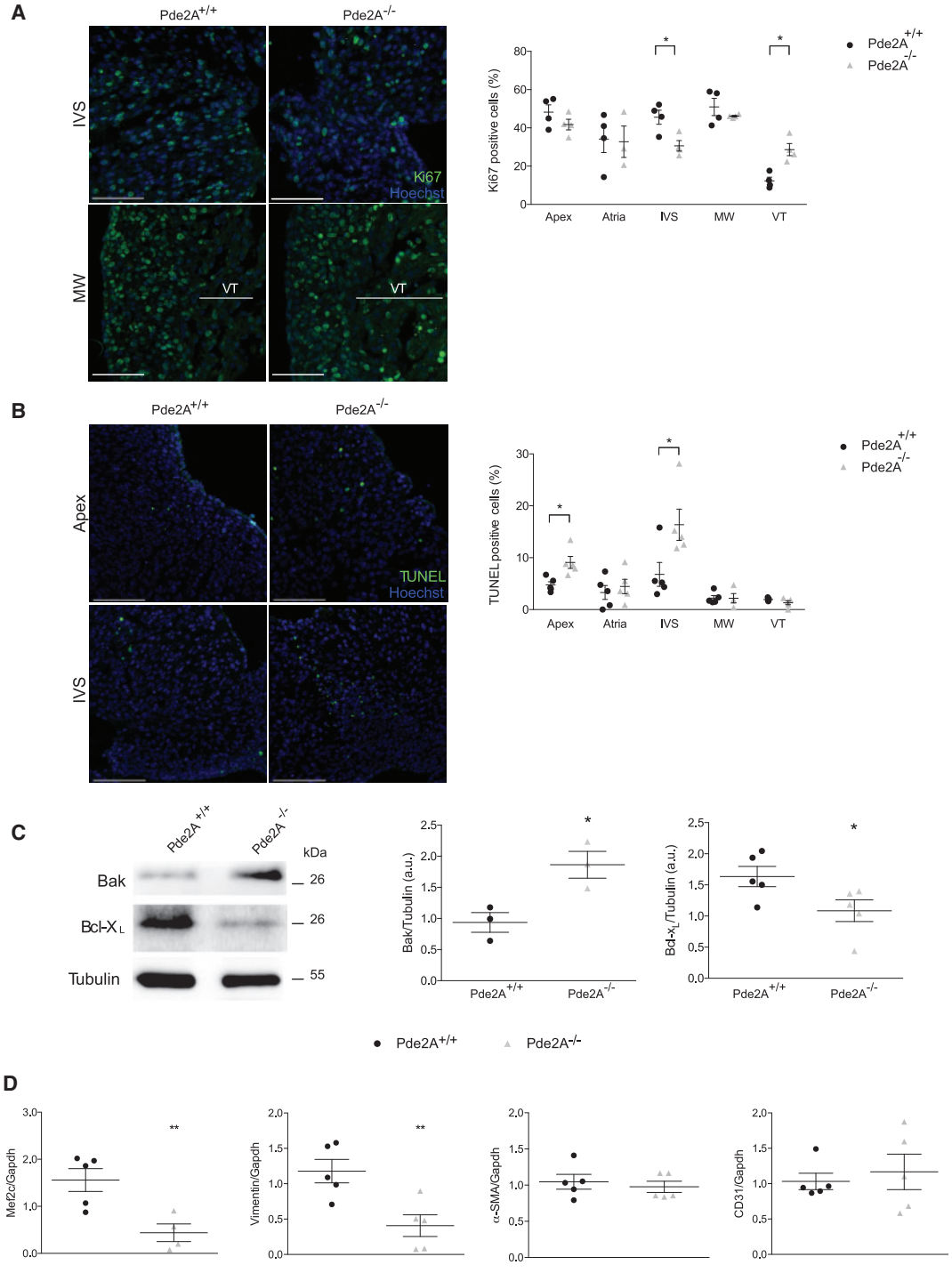

Figure 2 Interventricular septa of *Pde2A*$^{-/-}$ embryos show increased cellular apoptosis and reduced cell proliferation. (*A*) Representative images of immunofluorescence for Ki67 (green) proliferative marker performed on paraffin sections of E14.5 *Pde2A*$^{+/+}$ and *Pde2A*$^{-/-}$ hearts (IVS, MW and VT are shown). Scale bar: 50 μm. Quantification of cell proliferation is reported as percentage of Ki67-positive nuclei in the apex, atria, IVS, MW and VT in $n = 9–13$ sections from at least $n = 3$ embryos for each genotype; > 250 cells/field/heart. (*B*) Representative images of TUNEL staining (green) performed on paraffin sections of E14.5 *Pde2A*$^{+/+}$ and *Pde2A*$^{-/-}$ hearts (IVS and Apex are shown). Scale bar: 50 μm. Quantification of cell apoptosis is reported as percentage of TUNEL-positive nuclei in $n = 15–21$ sections from at least $n = 3$ embryos for each genotype; > 250 cells/field/heart. (*C*) Western blot analysis on protein extracts from E14.5 *Pde2A*$^{+/+}$ and *Pde2A*$^{-/-}$ hearts. Densitometry of Bak and Bcl-X_L protein expression relative to Tubulin is reported. Data are presented as dot plots of at least $n = 3$ hearts. (*D*) qRT–PCR expression levels of specific cell lineage markers on E14.5 *Pde2A*$^{+/+}$ and *Pde2A*$^{-/-}$ hearts. Dot plots represent relative expression levels for each analyzed gene. *Gapdh* was used as housekeeping gene for normalization. mRNA was analyzed on at least $n = 4$ hearts for each genotype. The mean value ± SEM is shown and Student's *t*-test was used for statistical analysis. *P<0.05 and **P<0.01.

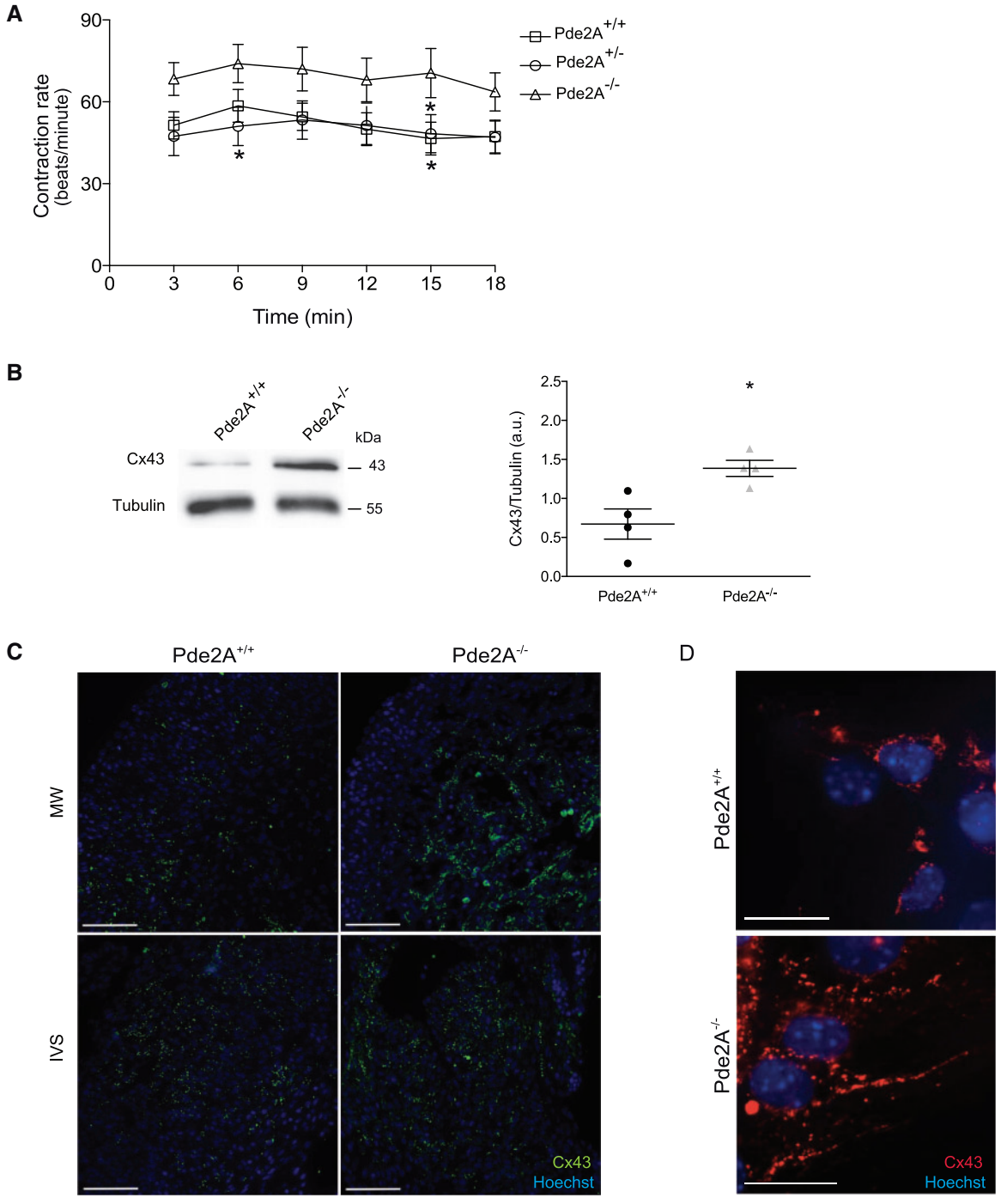

Figure 3 Analysis of contraction rate measured in spontaneous beating syncytia and Cx43 expression. (*A*) Contraction rate of cardiomyocyte cultures from E14.5 *Pde2A*$^{+/+}$, *Pde2A*$^{+/-}$, and *Pde2A*$^{-/-}$ hearts were recorded after a 3 min equilibration before period. Data are reported as $n = 8$ experiments performed in different cardiomyocyte preparations. The mean value ± SEM is shown and two-way ANOVA with Bonferroni post hoc test was used for statistical analysis. *$P < 0.05$. (*B*) Western blot analysis on protein extracts from E14.5 *Pde2A*$^{+/+}$ and *Pde2A*$^{-/-}$ hearts. Densitometry of Cx43 relative to Tubulin is shown. Data are reported as dot plots of $n = 4$ hearts for each genotype. The mean value ± SEM is shown and Student's *t*-test was used for statistical analysis. *$P < 0.05$. (*C*) Immunofluorescence of Cx43 (green) on E14.5 heart sections of *Pde2A*$^{+/+}$ and *Pde2A*$^{-/-}$ embryos. IVS and MW are shown. Scale bar: 50 µm. Images are representative of $n = 3$ embryonic hearts for each genotype. (*D*) Immunofluorescence of Cx43 (red) in cardiomyocytes isolated from E14.5 *Pde2A*$^{+/+}$ and *Pde2A*$^{-/-}$ embryos. Scale bar: 10 µm.

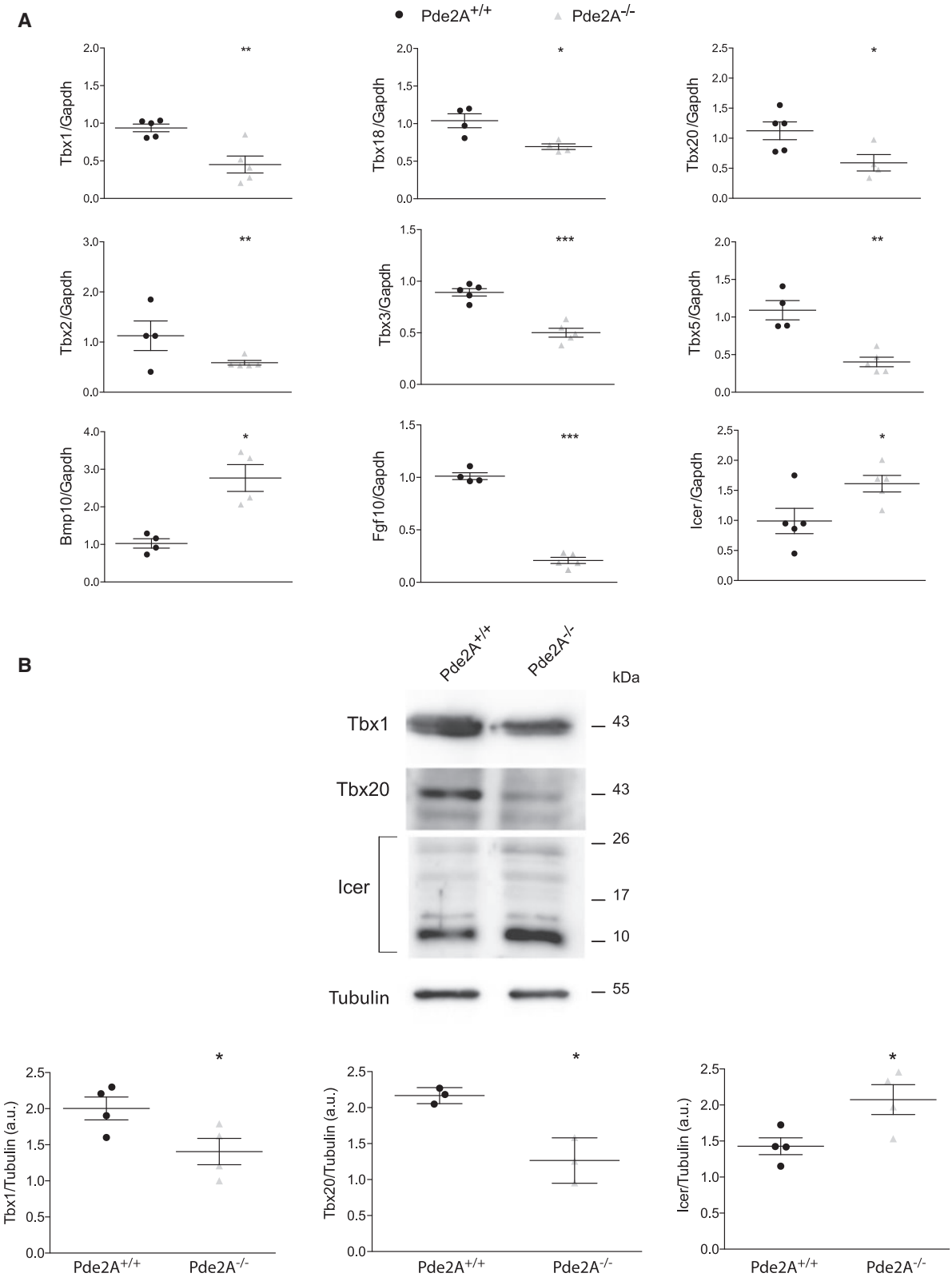

Figure 4 CHD-related genes showed a reduced expression pattern in hearts of *Pde2A*$^{-/-}$ embryos. (*A*) qRT–PCR expression levels of CHD-related genes on E14.5 *Pde2A*$^{+/+}$ and *Pde2A*$^{-/-}$ hearts. Dot plots represent relative expression levels for each analyzed gene. *Gapdh* was used as the housekeeping gene for normalization. mRNA was extracted from $n = 4$–5 hearts for each genotype. (*B*) Western blot analysis on protein extracts from E14.5 *Pde2A*$^{+/+}$ and *Pde2A*$^{-/-}$ hearts. Densitometry of Tbx1, Tbx20 and Icer relative to Tubulin is reported. Data are reported as dot plots of at least $n = 3$ hearts for each genotype. The mean value ± SEM is shown and Student's *t*-test was used for statistical analysis. *$P < 0.05$, **$P < 0.01$, ***$P < 0.001$.

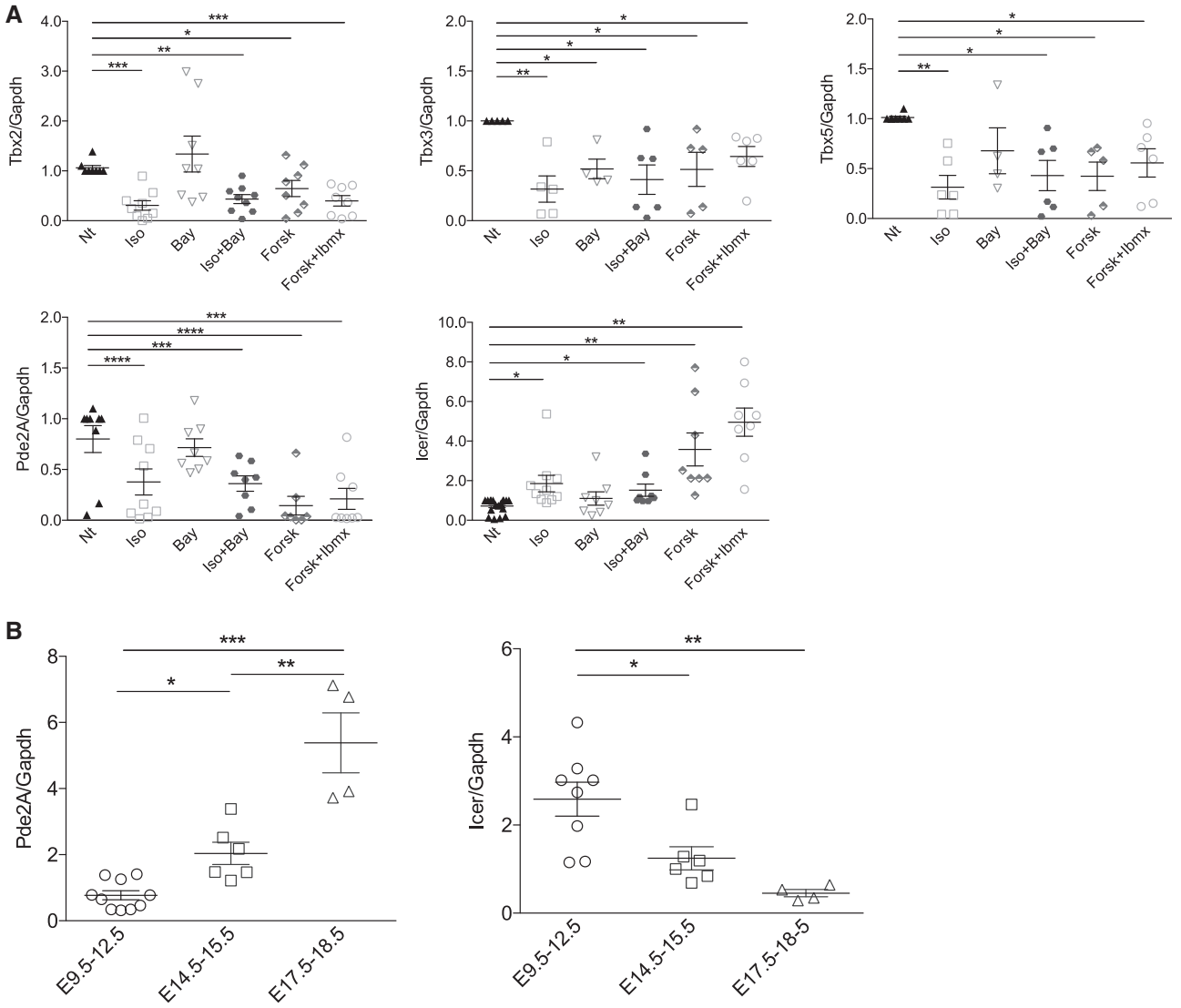

Figure 5 cAMP inducers modulate *Tbx* and *Pde2A* gene expression. (*A*) qRT–PCR products for *Tbx2*, *Tbx3*, *Tbx5*, *Icer* and *Pde2A* in wild-type cardiac cells isolated from E14.5 hearts cultured for 48 h in the presence of 10 µmol/L Bay 60-7550 and/or 10 µmol/L Iso, 10 µmol/L Forsk and 10 µmol/L Forsk/IBMX. Nt = not treated. Dot plots represent normalized expression levels for each analyzed gene. At least $n = 4$ cardiac cell preparations. (*B*) qRT–PCR expression levels of *Pde2A* and *Icer* on wild-type E9.5- E18.5 hearts. Dot plots represent relative expression levels for each analyzed gene. *Gapdh* was used as housekeeping gene for normalization. mRNA was extracted from at least $n = 4$ hearts for each range of development. The mean value ± SEM is shown and one-way ANOVA with Bonferroni post hoc Test was used for statistical analysis. *$P < 0.05$, **$P < 0.01$, ***$P < 0.001$ and ****$P < 0.0001$.

which stimulates cAMP synthesis by binding to β-adrenergic receptors. qRT–PCR analyses on selected *Tbx* genes showed that Iso stimulation induced a decrease in *Tbx2*, *Tbx3* and *Tbx5* mRNA levels (*Figure 5A*). Similar decreases were observed after Iso stimulation with the Pde2A inhibitor, whereas Pde2A inhibitor alone only down-regulated *Tbx3* expression level (*Figure 5A*). To further evaluate if *Tbx* gene expression was also modulated by increasing cAMP production independent of β-adrenergic stimulation, experiments were performed by using forskolin (Forsk) and 3-Isobutyl-1-methylxanthine (IBMX), a cAMP inducer and a pan-Pde inhibitor, respectively. Both Forsk and Forsk + IBMX treatments down-regulated Tbx genes. These results suggest that a robust increase in cAMP is responsible for *Tbx* gene down-regulation and indicates that Pde2A activity may modulate the expression of *Tbx* genes. Since *Pde2A* knockout hearts showed Icer up-regulation, mRNA levels of *Pde2A* and *Icer* were measured in treated cardiomyocyte cultures. *Icer* and *Pde2A* mRNAs were, respectively, up-regulated and down-regulated by Iso, Forsk and Forsk + IBMX stimulations (*Figure 5A*). Altogether these results suggest a cAMP dependent down-regulation of *Tbx* and *Pde2A* genes possibly through Icer up-regulation. To further investigate the possible correlation between *Pde2A* and *Icer*, their mRNA levels were analyzed during cardiac development (*Figure 5B*). *Pde2A* mRNA increased during cardiac development, whereas *Icer* transcript was

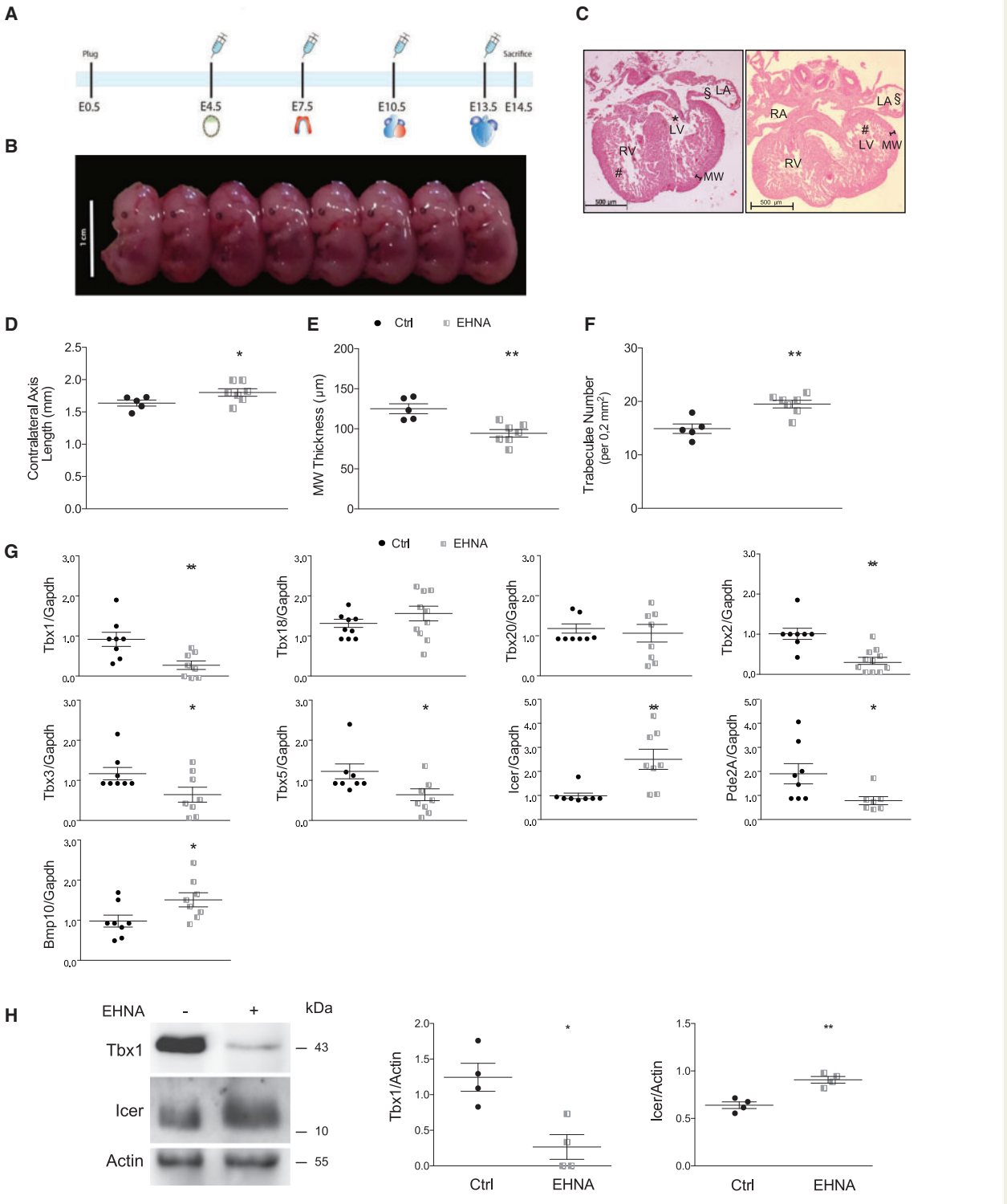

Figure 6 CHD defects in Pde2A-inhibited mice. (*A*) Timeline of EHNA injections during embryogenesis from E4.5 to E13.5. (*B*) Picture of litters at E14.5 after EHNA treatment. Total $n = 23$ embryos were analyzed from three pregnant females. (*C*) Hematoxylin & Eosin staining of E14.5 hearts after EHNA treatment showing similar morphological defects of *Pde2A*$^{-/-}$ embryos. * indicates incomplete formation of the IVS; § indicates the absence of trabeculation in the atria, black bar indicates the thickness of compact myocardium and # indicates hypertrabeculation. (*D–F*) Dot plots showing the contralateral axis (*D*), the MW thickness (*E*) and the trabeculae number (*F*). Dots represent the analysis of 30 sections/embryo. The trabeculae number was quantified in $n = 48$ fields of 0.2 mm^2/24 sections. Ctrl ($n = 5$) and EHNA-treated ($n = 7$) embryos were analyzed. (*G*) qRT–PCR analysis of CHD-related genes after EHNA treatment *in vivo* in embryonic hearts. Dot plots represent relative expression levels for each analyzed gene. *Gapdh* was used as housekeeping gene for normalization. mRNA was extracted from at least $n = 7$ hearts of Ctrl and EHNA-treated embryos. (*H*) Western blot of Tbx1 and Icer on protein extracts from hearts of Ctrl and EHNA treated embryos. Densitometry relative to Actin is shown, $n = 4$ hearts were analyzed. The mean value ± SEM is shown and Student's *t*-test was used for statistical analysis. *$P < 0.05$, **$P < 0.01$.

Table 3 Penetrance and Fisher's exact test of congenital heart defects observed in E14.5 embryos after EHNA treatment ($n = 13$)

	Defects (%)	Fisher's test (vs control)
ASD	15.4	0.48
Smooth Atria	23.1	0.22
VSD	61.5	0.0016**
Ventricular hypertrabeculation	84.6	0.0001***
Wall noncompaction	38.46	0.040*
AO	12.5	1.0

ASD, atrial septal defects; VSD, ventricular septal defects; AO, overriding aorta; DORV, double outlet right ventricle; OFTD, outflow tract defect.
*$P < 0.05$.
**$P < 0.01$.
***$P < 0.001$.

down-regulated, further suggesting the instauration of a negative feedback loop, similarly to what was reported for Pde3A/Icer system.[31]

3.7 Pde2A inhibition recapitulates embryonic heart defects *in vivo*

To test whether Pde2A activity directly induces heart defects during embryogenesis, *Pde2A*$^{+/+}$ pregnant females were injected with 0.03 mg/kg EHNA after blastula implantation following the timeline represented in *Figure 6A*. Embryos were collected at E14.5 and no evident gross phenotypes, such as nuchal edema, hemorrhages or small liver were observed (*Figure 6B*). Interestingly, histological sections of embryonic hearts after EHNA treatment showed IVS defects, hypertrabeculation and noncompaction phenotype (*Figure 6C* and *D–F*, *Table 3*). The expression pattern of cardiac genes involved in heart development was very similar in hearts of *Pde2A*$^{-/-}$ and Pde2A-inhibited embryos. *Bmp10* and *Icer* were up-regulated and most of *Tbx* genes were down-regulated as shown by qRT–PCR and protein analyses (*Figure 6G* and *H*). *Pde2A* expression was decreased by 50% c in EHNA-treated hearts, compared to the levels in untreated hearts (*Figure 6G*), confirming the results obtained in the *in vitro* experiments. Altogether these results demonstrate that Pde2A is a master regulator of fetal heart development modulating *Tbx* gene expression through the activation of the cAMP-dependent repressor Icer.

3.8 Pde2A is required in the early and late phase of heart development

Next, it was evaluated whether Pde2A is required in the early phase of heart development and/or it is involved in later heart remodelling and growth. EHNA was administered as shown in the timeline of *Figure 7A*. Mice receiving treatment I had EHNA injected from E4.5 of pregnancy until E10.5; while mice receiving treatment II had EHNA administered from E10.5 until E13.5. All embryos were collected at E14.5. If Pde2A is required in the early stage of heart development treatment I should recapitulate the phenotype of *Pde2A*$^{-/-}$embryos; on the contrary, if Pde2A controls fetal heart growth treatment II would then recapitulate the CHDs observed in *Pde2A*$^{-/-}$ embryos. Indeed, full recapitulation of major *Pde2A*$^{-/-}$ heart defects was found to occur after treatment I in more than 60% of the embryos analyzed, whereas few defects, such as contralateral axis increase, were observed after treatment II (*Figure 7B* and *C*).

These results prompted us to investigate some specific lineage markers of cardiac progenitors of primary (*c-Kit*) and secondary (*Islet1*) heart fields and of neural crest cells (*Sox9*) after treatments I and II. As shown in *Figure 7D*, the expression of the *c-Kit* marker was strongly reduced after both treatments, whereas *Islet1*and *Sox9* were decreased only after treatment I. To further investigate the role of Pde2A in early cardiogenesis, embryos were analyzed at E9.5. The effects of Pde2A absence on cardiac cell apoptosis and proliferation were evaluated in the hearts, outflow tract and dorsal pericardial region of E9.5 embryos (*Figure 8A*). As shown in *Figure 8A-B*, apoptosis was increased in cardiac Islet1-positive cells and AP2α-positive neural crest cells. Proliferation was not affected in these cell populations by the absence of PDE2 (data not shown).

Similarly to what it was observed at E14.5, *c-Kit*, *Islet1* and *Sox9* transcripts were down-regulated in the absence of Pde2A at developmental stage E9.5 (*Figure 8C*). The cardiomyocyte marker, cTnI was also down-regulated at this embryonic age (*Figure 8D*). *Tbx1 and 2* genes and *Icer* were not modulated in *Pde2A*$^{-/-}$ embryos (*Figure 8E*). Altogether, these data delineate a dual/differential role of Pde2A in early and late cardiogenesis.

4. Discussion

Pde2A knockout mice die by E15.5, displaying nuchal edema, anemia, diffuse hemorrhages and an extremely reduced liver size that could lead to the observed embryonic lethality. Nuchal edema is often associated with cardiac malformations[8,17,24,32–34] and, in this paper, we reported that Pde2A is indispensable for heart development because *Pde2A* knockout embryos show severe atria and ventricular defects.

4.1 Morphological, cellular and functional defects in hearts of Pde2A knockout mice

Pde2A$^{-/-}$ mice die after the formation of the four heart chambers is complete. Molecular analyses indicated that early cardiac progenitors from the second heart field and neural crest are affected by Pde2A deficiency. It is noteworthy that, despite the expression of many different Pdes in the heart,[20] none of them is able to functionally compensate for Pde2A absence. Hearts of *Pde2A*$^{-/-}$ fetuses show cardiac deformities. A smooth appearance of atrial wall suggests that pectinate muscles are not formed,[35] *Pde2A*$^{-/-}$ fetuses do not completely develop the IVS, show ventricular enlargement, present ventricular hypertrabeculation, and in most of the embryos, MW noncompaction was observed. To some extent they also show atrial septal defects, overriding aorta, double-outlet right ventricle, valves and outflow tract defects. Similar abnormalities have been extensively reported in human CHDs[2,32,33,36]

The enlarged contralateral axis observed in *Pde2A*$^{-/-}$ hearts could be due to hypertrophy of the ventricular wall and/or to a dilated myopathy. The ventricular wall of hearts of *Pde2A*$^{-/-}$ mice was significantly thinner than the cardiac wall of heterozygous and wild-type littermates supporting the hypothesis that the ventricles of *Pde2A* knockout mice are affected by dilated myopathy.

To understand the causes of the observed cardiac defects at tissue and cellular levels, proliferation, survival and growth of cardiomyocytes were investigated in *Pde2A* knockout mice. Proliferative and apoptotic assays displayed decreased cardiomyocyte proliferation in

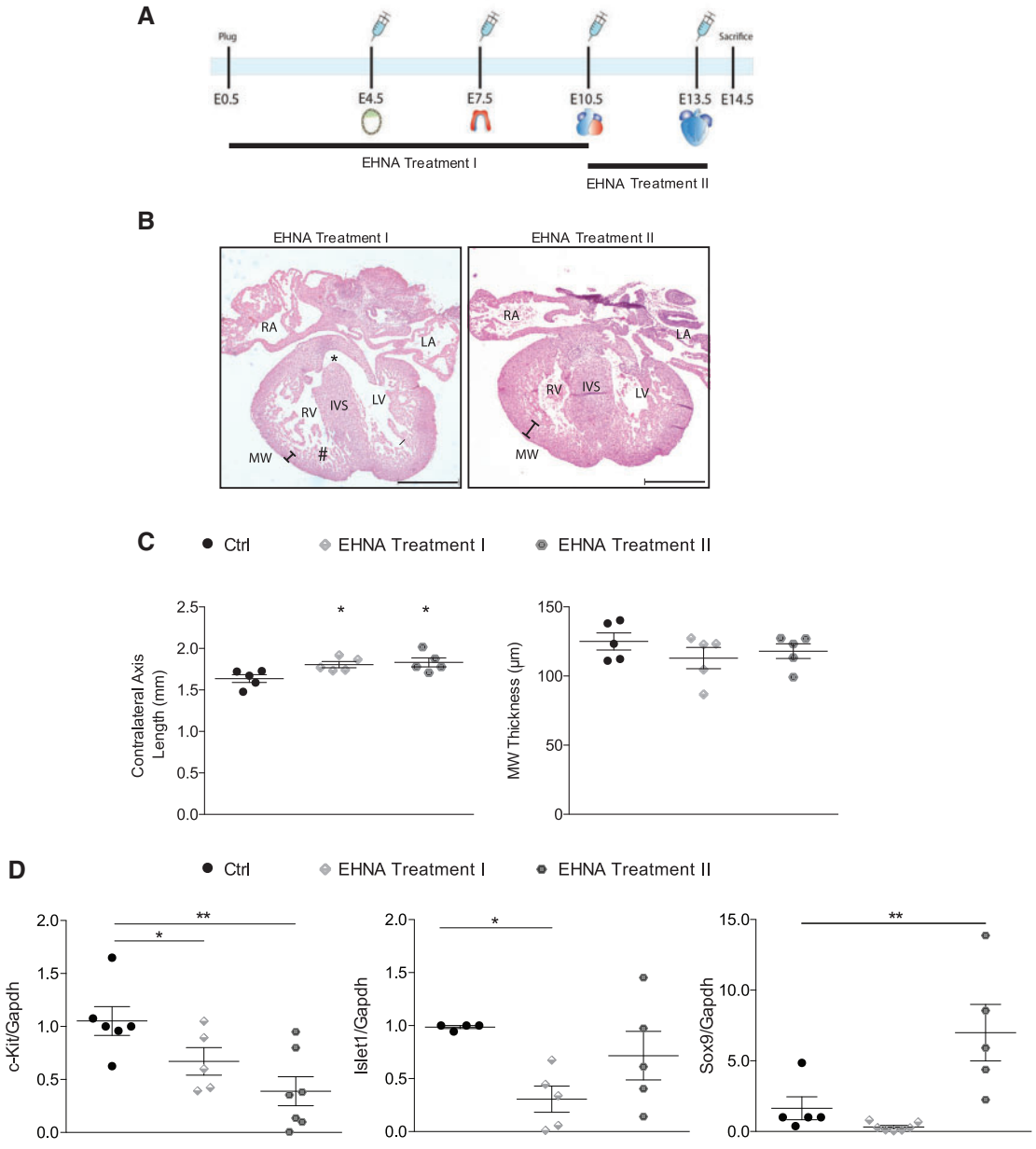

Figure 7 Pde2A inhibition affects cardiac progenitor cells. (*A*) Timeline of EHNA treatment I and II. (*B*) Hematoxylin & Eosin staining of E14.5 hearts after EHNA treatments I and II. * indicates incomplete formation of the IVS, black bar indicates the thickness of MW and # indicates hypertrabeculation. (*C*) Dot plots showing the contralateral axis and the myocardium thickness in E14.5 hearts from five untreated and after EHNA-treated embryos. The mean value ± SEM is shown and Student's *t*-test vs. Ctrl was used for statistical analysis *P<0.05. (*D*) qRT–PCR expression levels of *c-Kit*, *Islet1* and *Sox9* genes in fetal hearts after EHNA treatment I and II. Dot plots represent relative expression levels for each analyzed gene. *Gapdh* was used as housekeeping gene for normalization. mRNA of at least $n = 4$ hearts was analyzed in each experiment. The mean value ± SEM is shown and one-way ANOVA with Bonferroni post hoc Test was used for statistical analysis. *$P < 0.05$, **$P < 0.01$.

IVS, increased Ki67 staining in VT region and increased cellular apoptosis in the proximity of membranous septum zone. The increment of cell death in the apex, explained the establishment of a dilated myopathy with a thinner ventricular wall and an enlarged ventricular cavity. A thinner ventricular wall together with the atria defects may also lead to diminished ejection fraction, a parameter that was not possible to evaluate in fetal mice. However, through *in vitro* experiments, it was observed that cardiomyocyte contraction rate was slightly affected by *Pde2A* deletion and mutant beating cardiomyocytes tend to arrest more frequently. Moreover, Cx43 was upregulated in *Pde2A* knockout mouse ventricles with no evident change in cellular localization. An increase in Cx43 expression was reported to induce electrical alteration of the conduction system with cardiac arrhythmias in Duchenne patients.[37] Noteworthy, several studies reported that an increase in

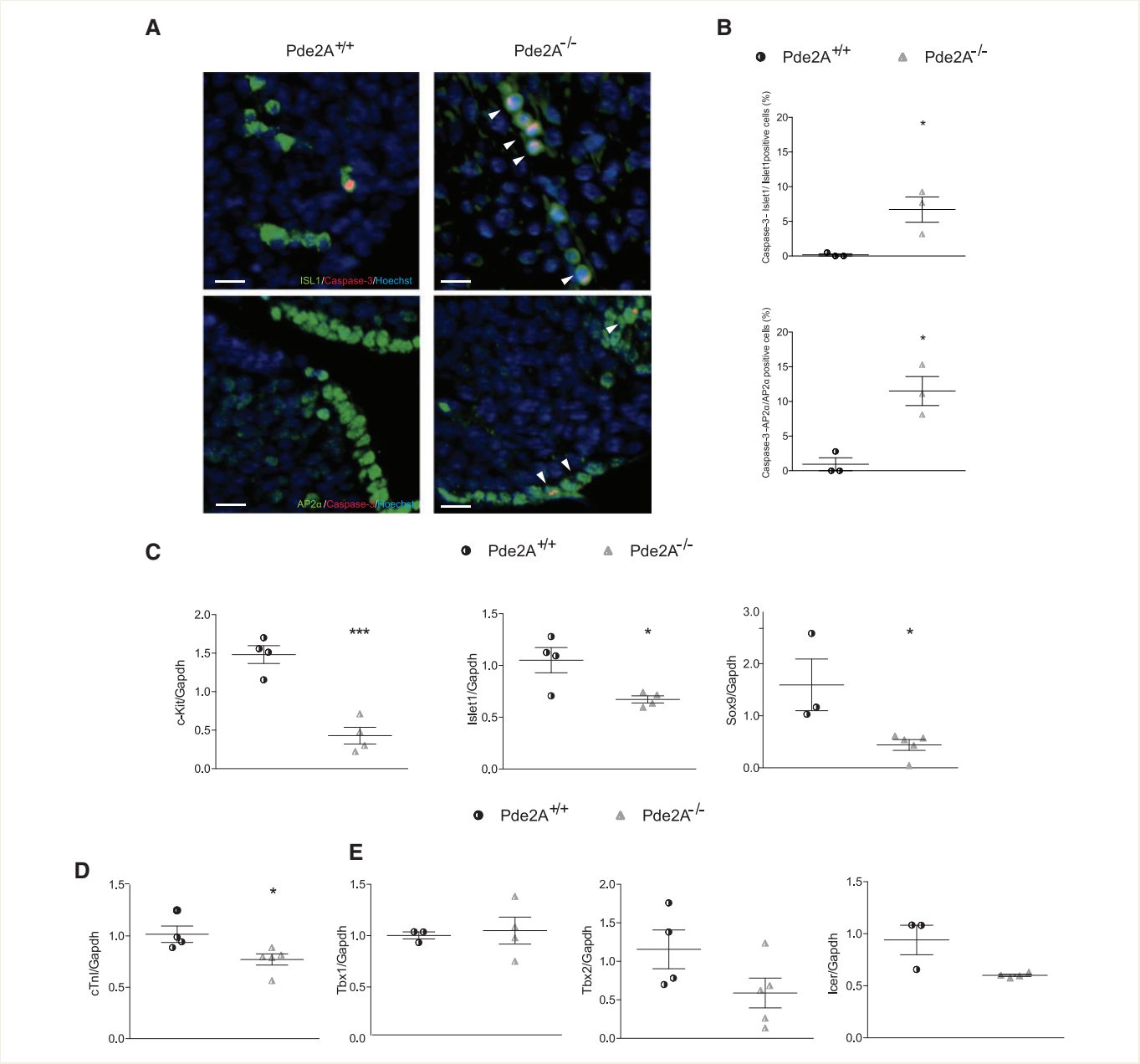

Figure 8 E9.5 *Pde2A*$^{-/-}$ embryos show cardiac progenitor and neural crest deployment. (*A*) Immunofluorescence on paraffin sections of *Pde2A*$^{\pm/\pm}$ and *Pde2A*$^{-/-}$ heart and dorsal region with Caspase-3 antibody (red) and Islet1 or AP2α (green) antibodies. Scale bar: 10 μm. Arrowheads indicate double positive cells. (*B*) Quantification analysis of Islet1-Caspase-3 and AP2α-Caspase3 double positive cells on total islet1 or AP2α positive cells, respectively, is shown. Dot plots represent the mean value of percentage of positive cells counted in $n = 3$ sections from $n = 3$ embryos for each genotype. (*C–E*) qRT–PCR analysis of specific markers for the heart fields, neural crest cells and cardiomyocytes in E9.5 *Pde2A*$^{\pm/\pm}$ and *Pde2A*$^{-/-}$ hearts. Dot plots represent relative expression levels for each analyzed gene. *Gapdh* was used as housekeeping gene for normalization. mRNA was analyzed on at least $n = 3$ hearts for each genotype. The mean value ± SEM is shown and Student's *t*-test was used for statistical analysis. *$P \leq 0.05$ and ***$P \leq 0.001$.

intracellular cAMP enhanced Cx43 gap junction assembly, number and size-mediated communication.[38–40] The effects of *Pde2A* deficiency on heart structure and function may be due to the increase in cAMP production that in turn causes a significant increase in Cx43 expression.

Trabeculae formation is a landmark in the initiation of ventricular chamber maturation[41] and the trabeculae contribute to the increase of myocardial mass.[42] The thickness and increased number of trabeculae that were observed in hearts of *Pde2A*$^{-/-}$ mice, could be associated to an increase in cell proliferation. Indeed, an increase in cell proliferation was observed in trabeculae of *Pde2A*$^{-/-}$ hearts and the molecular analyses revealed that Bmp10 was up-regulated in *Pde2A* knockout heart. Bmp10 is a growth factor associated to proliferation of cardiomyocytes in the trabecular wall and its expression is required for trabeculae formation.[27] In mouse models of human CHDs, highest number and enlarged size of VT are associated with Bmp10 up-regulation,[8,43] as was

observed in *Pde2A* knockout hearts, supporting the correlation between Pde2A deficiency and congenital heart disease in mice.

4.2 Pde2A deficiency affects expression of *Tbx* cardiac specific lineage genes

We then evaluated whether Pde2A has a critical role modulating the expression of genes which regulate cardiac development. Cardiac malformations of *Pde2A* knockout embryos were associated to a transcript reduction of all *Tbx* genes and their targets in fetal stage. Several studies reported that deletion or loss of function mutations of these genes cause heart defects like those observed in *Pde2A* knockout mice. *Tbx1* knockout mice fail to form the IVS and die at the time of birth.[44,45] As a target gene of Tbx1,[28] *Fgf10* is required for normal heart development by promoting fetal cardiomyocyte proliferation in the MW.[46] Tbx18 expression is associated with the formation of the cardiac venous pole and its presence was suggested to contribute to IVS and the left ventricle formation. Mice with complete loss of Tbx20 can develop a linear heart tube but heart looping and chamber formation do not occur; *Tbx20* heterozygous mice show onset of a dilated cardiomyopathy similar to a subset of the human defects.[47,48] *Tbx2* and *Tbx3* are two closely related transcription factor genes of *Tbx2* subfamily. They are exclusively associated with non-chamber myocardium of the atrioventricular canal (*Tbx2* and *Tbx3*) and outflow tract (*Tbx2*) during cardiac development.[47] Tbx2 acts as repressor of chamber genes in the atrioventricular region of myocardium.[49] Both of them were robustly down-regulated in *Pde2A* mutant mice, however e heart cavities develop in the absence of Pde2A, we might assume that the remaining Tbx2 and Tbx3 levels are sufficient for chamber formation, although they might cause the outflow tract defects observed in some *Pde2A* null hearts. However, we cannot exclude that these defects may be caused by other genes. For instance, other than *Tbx1* and *Tbx2*, also loss of *Mef2c* function from anterior secondary heart field resulted in a spectrum of outflow tract alignment defects, ranging from overriding aorta to double-outlet right ventricles.[50] *Mef2c* was down-regulated in *Pde2A* knockout hearts. Further experiments will be done to deeply understand the nature of the cellular and molecular defects of *Pde2A* knockout.

Intriguingly, Cx43 that is normally inhibited by Tbx2,[51] was up-regulated in *Pde2A*$^{-/-}$ hearts, strengthening the hypothesis that Pde2A modulates *Tbx2* gene expression. Finally, *Tbx5* is associated with VSD, noncompact myocardium wall and hypertrabeculation[52] and it was strongly reduced in *Pde2A* knockout mice. Altogether these data suggest that Pde2A modulates the expression of several members of Tbx family and other transcription factors related to many cardiac defects found in CHDs.

4.3 Pde2A activity is responsible of fetal heart defects and correlates with *Icer* increase and *Tbx* decrease

Pde2A plays an important role degrading the cAMP pool and preventing cAMP signalling pathways in cardiomyocytes,[20] but no information was previously available on its role in cardiac development.

An increase in cAMP was detected in E14.5 hearts of *Pde2A* knockout embryos, which can induce a constitutive activation of cAMP-dependent transcription factors and repressors. To test this hypothesis, the expression level of Icer, a cAMP-dependent repressor was evaluated in the hearts of *Pde2A* deficient mice. *Icer* mRNA was up-regulated either in fetal hearts of both *Pde2A*$^{-/-}$ and EHNA-treated embryos. Moreover, *Pde2A* levels were found down-regulated in Pde2A inhibited cardiomyocytes and mice. These findings are very similar to what it has been shown for Pde3A inhibition, which activates cAMP/PKA signalling and up-regulates Icer that in turn represses Pde3A gene transcription,[31] suggesting an analogous autoregulatory feedback for Pde2A. In this regard, it would be interesting to evaluate whether changes in cAMP levels affects expression of other Pdes and the cross-talk between cAMP/cGMP nucleotides.

To investigate the direct role of cAMP in Tbx expression, cells from E14.5 wild-type embryos were isolated and cultured in the presence of a selective Pde2A inhibitor and/or adenylate cyclase activators. At basal condition, Bay 60-7550 inhibitor was able to significantly reduce *Tbx3* expression and cause a downward trend of other *Tbx* genes. However, when cAMP levels were increased by Iso, Forsk or Forsk + IBMX stimulations *Tbx2*, *Tbx3* and *Tbx5* down-regulation was observed and notably up-regulation of *Icer* was detected. After Pde2A inhibition *in vivo*, *Tbx*, *Icer* and *Pde2A* transcript modulation was observed probably because a critical threshold for cAMP level was reached in these conditions. These results show for the first time that intracellular cAMP elevation in the cardiomyocytes of developing heart is fundamental for the inhibition of Tbx expression and the establishment of CHD.

Intriguingly, high affinity CRE-binding sites are present in the promoters of *Tbx* genes (see MatInspector software at http://www.genomatix.de) strengthening the hypothesis that induction of *Icer* by the rise of cAMP might represses *Tbx* expression in fetal hearts.

In E9.5 hearts of wild-type mice, PDE2A mRNA is present at very low level and this might explain why Tbx1, Tbx 2 and Icer are not modulated in knockout embryos compared to their expression in the hearts of wild-type embryos. Since Tbx 1, Tbx 2 and Icer are not modulated by cAMP/PDE2 dependent pathways, in the E9.5 hearts their expression may depend by other molecular determinants for cardiac development like Bmp2 and Bmp4[29,53,54] and by Notch signalling.[30]

4.4 Pde2A functions in early and late heart development

We have found that Pde2A is always expressed in the heart, but its level increases during embryogenesis, indicating a potential role all over the stage of heart development. To study the exact embryonic stage at which Pde2A is required for heart development, different approaches were employed. Pde2A inhibition *in vivo* from E4.5 until E10.5 recapitulated the morphological abnormalities and molecular alteration of the first and second heart field observed in null embryos at E14.5, indicating that Pde2A is indispensable in the early phase of cardiogenesis. Some heart defects were observed when Pde2A was inhibited after E10.5 suggesting also a late role of Pde2A in heart development which correlates with *Mef2c* down-regulation in *Pde2A* knockout embryos. Increase in apoptosis and decrease in cardiomyocyte differentiation were observed at E9.5 in *Pde2A*$^{-/-}$ mice, which could be due to the significant decrease in specific markers of neural crest precursors and early cardiogenesis such as Sox9, c-Kit, Islet. Cardiac cell proliferation defects and alteration of *Tbx* gene expression were instead observed exclusively at later stages of heart development.

In conclusion, the impairment of early cardiac progenitor cells in the first and second heart fields might explain the CHDs of *Pde2A* deficient embryos, such as atrial and ventricular septal defects, whereas late gene expression alterations might explain the CHDs including impairment of cardiac growth, non-compaction and cardiomyocyte beating.

4.5 Study limitations and perspectives

Our observations uncover a novel and critical role of Pde2A on cardiac development and in particular on heart chamber septation and heart wall maturation. We pointed out a direct effect of Pde2A/cAMP on cardiomyocyte differentiation and survival, however we cannot exclude an indirect effect on endothelial, smooth muscle, fibroblast and blood cells; subjects of future investigation. Conditional *Pde2A* models are necessary to clarify the cell-specific function of Pde2A and its role in the cell-to-cell interaction. Our data support the hypothesis that increased Icer expression in *Pde2A*-deficient mice down-regulates *Tbx* gene expression, however future experiments will dissect whether Icer directly binds *Tbx* genes to promote their down-regulation. cAMP/PKA modulates a plethora of molecular targets that deserves further investigations; indeed intracellular Ca^{2+} signalling might be affected in $Pde2A^{-/-}$ cardiomyocytes, giving an explanation for the beating and connexins alteration. Expression, activity and compartmentalization of other Pde families in *Pde2A* knockout hearts needs also to be clarified in the future work. Furthermore, our study might give new insights to the recent debate on the role of Pde2A in cardiac hypertrophy and heart failure.[55,56]

No CHDs associated to *Pde2A* mutations in humans have been reported up to date. Since defects of atrial and ventricular septation are the most common type of CHDs, it will be interesting to determine how frequently mutations in *Pde2A* gene are associated with CHDs in humans. In mice only the complete ablation of Pde2A is critical for heart embryonic development, however this does not rule out the possibility that differential dosage/activity of Pde2A plays a role in development of the human heart by decreasing TBX1 dosage[57] or that other somatic mutations negatively synergize with hypomorphic *Pde2A* mutations.

Acknowledgements

We thank EMMA service project that founded the EC FP7 Capacities Specific Program and allowed us to obtain $Pde2A^{+/-}$ mice. The Islet1 antibody (DSHB-40.2D6 Iowa City, Iowa) developed by David R. Soll, c/o DSHB, at The University of Iowa was obtained from the Developmental Studies Hybridoma Bank, created by the NICHD of the NIH and maintained at The University of Iowa, Department of Biology, Iowa City, IA. We are particularly thankful to Giulia D'Amati and Francesco Carlomagno, Sapienza University, Italy for helping on histological examination and analyses, Elena Vicini, Sapienza University, Italy for instruments sharing, Lucia Monaco, Sapienza University, Italy for reagent sharing, Valentina Fustaino IBCN-CNR, Italy for statistical analyses and Danilo Federici, Sapienza University, Italy for helping on murine colony maintenance. We thank Hiba Komati, Ottawa University, Canada for the critical reading of the manuscript and Toni West, University of California Davis, USA for editing grammar and syntax.

Supplementary material

Supplementary material is available at *Cardiovascular Research* online.

Funding

This work was supported by research grants from 'Istituto Nazionale Assicurazione Infortuni sul Lavoro' [INAIL 2010 to AL and FN], from University of Sapienza [Ateneo 2009 and Progetti Medi 2017 to FN] and from 'Italian Ministry of University' [FIRB 2010 RBAP109BLT, RBFR10URHP to AL and FN; PRIN 2010 KL2Y73-006 to FN; FIRB 2012 RBFR12FI27 to FB; SIR RBSI149K2N 000315_15 to FB; PRIN 2012 prot. 2012227FLF to MP].

Conflict of interest: none declared.

References

1. Bjornard K, Riehle-Colarusso T, Gilboa SM, Correa A. Patterns in the prevalence of congenital heart defects, metropolitan Atlanta, 1978 to 2005. *Birth Defects Res Part A Clin Mol Teratol* 2013; **97**:87–94.
2. Hoffman JI, Kaplan S. The incidence of congenital heart disease. *J Am Coll Cardiol* 2002; **39**:1890–1900.
3. D'Alto M, Mahadevan VS. Pulmonary arterial hypertension associated with congenital heart disease. *Eur Respir Rev* 2012; **21**:328–337.
4. Rajdev A, Garan H, Biviano A. Arrhythmias in pulmonary arterial hypertension. *Prog Cardiovasc Dis* 2012; **55**:180–186.
5. Penny DJ, Vick GW III. Ventricular septal defect. *Lancet* 2011; **377**: 1103–1112.
6. Soufflet V, Van de Bruaene A, Troost E, Gewillig M, Moons P, Post MC, Budts W. Behavior of unrepaired perimembranous ventricular septal defect in young adults. *Am J Cardiol* 2010; **105**: 404–407.
7. McCulley DJ, Black BL. Transcription factor pathways and congenital heart disease. *Curr Top Dev Biol* 2012; **100**: 253–277.
8. Chen H, Zhang W, Li D, Cordes TM, Mark Payne R, Shou W. Analysis of ventricular hypertrabeculation and noncompaction using genetically engineered mouse models. *Pediatr Cardiol* 2009; **30**:626–634.
9. Pignatelli RH, McMahon CJ, Dreyer WJ, Denfield SW, Price J, Belmont JW, Craigen WJ, Wu J, El SH, Bezold LI, Clunie S, Fernbach S, Bowles NE, Towbin JA. Clinical characterization of left ventricular noncompaction in children: a relatively common form of cardiomyopathy. *Circulation* 2003; **108**:2672–2678.
10. Savolainen SM, Foley JF, Elmore SA. Histology atlas of the developing mouse heart with emphasis on E11.5 to E18.5. *Toxicol Pathol* 2009; **37**:395–414.
11. Mikawa T, Gourdie RG. Pericardial mesoderm generates a population of coronary smooth muscle cells migrating into the heart along with ingrowth of the epicardial organ. *Dev Biol* 1996; **174**:221–232.
12. Conway SJ, Kruzynska-Frejtag A, Kneer PL, Machnicki M, Koushik SV. What cardiovascular defect does my prenatal mouse mutant have, and why? *Genesis* 2003; **35**: 1–21.
13. Christoffels VM, Burch JB, Moorman AF. Architectural plan for the heart: early patterning and delineation of the chambers and the nodes. *Trends Cardiovasc Med* 2004; **14**:301–307.
14. Buckingham M, Meilhac S, Zaffran S. Building the mammalian heart from two sources of myocardial cells. *Nat Rev Genet* 2005; **6**:826–835.
15. Plageman TF Jr, Yutzey KE. T-box genes and heart development: putting the "T" in heart. *Dev Dyn* 2005; **232**:11–20.
16. Hoogaars WM, Barnett P, Moorman AF, Christoffels VM. T-box factors determine cardiac design. *Cell Mol Life Sci* 2007; **64**:646–660.
17. Merscher S, Funke B, Epstein JA, Heyer J, Puech A, Lu MM, Xavier RJ, Demay MB, Russell RG, Factor S, Tokooya K, Jore BS, Lopez M, Pandita RK, Lia M, Carrion D, Xu H, Schorle H, Kobler JB, Scambler P, Wynshaw-Boris A, Skoultchi AI, Morrow BE, Kucherlapati R. TBX1 is responsible for cardiovascular defects in velo-cardio-facial/DiGeorge syndrome. *Cell* 2001; **104**:619–629.
18. Li QY, Newbury-Ecob RA, Terrett JA, Wilson DI, Curtis AR, Yi CH, Gebuhr T, Bullen PJ, Robson SC, Strachan T, Bonnet D, Lyonnet S, Young ID, Raeburn JA, Buckler AJ, Law DJ, Brook JD. Holt-Oram syndrome is caused by mutations in TBX5, a member of the Brachyury (T) gene family. *Nat Genet* 1997; **15**:21–29.
19. Stephenson DT, Coskran TM, Wilhelms MB, Adamowicz WO, O'Donnell MM, Muravnick KB, Menniti FS, Kleiman RJ, Morton D. Immunohistochemical localization of phosphodiesterase 2A in multiple mammalian species. *J Histochem Cytochem* 2009; **57**:933–949.
20. Isidori AM, Cornacchione M, Barbagallo F, Di Grazia A, Barrios F, Fassina L, Monaco L, Giannetta E, Gianfrilli D, Garofalo S, Zhang X, Chen X, Xiang YK, Lenzi A, Pellegrini M, Naro F. Inhibition of type 5 phosphodiesterase counteracts beta2-adrenergic signalling in beating cardiomyocytes. *Cardiovasc Res* 2015; **106**:408–420.
21. Acin-Perez R, Russwurm M, Gunnewig K, Gertz M, Zoidl G, Ramos L, Buck J, Levin LR, Rassow J, Manfredi G, Steegborn C. A phosphodiesterase 2A isoform localized to mitochondria regulates respiration. *J Biol Chem* 2011; **286**:30423–30432.
22. Sassone-Corsi P. Coupling gene expression to cAMP signalling: role of CREB and CREM. *Int J Biochem Cell Biol* 1998; **30**:27–38.
23. Molina CA, Foulkes NS, Lalli E, Sassone-Corsi P. Inducibility and negative autoregulation of CREM: an alternative promoter directs the expression of ICER, an early response repressor. *Cell* 1993; **75**:875–886.
24. Fassina L, Di Grazia A, Naro F, Monaco L, De Angelis MG, Magenes G. Video evaluation of the kinematics and dynamics of the beating cardiac syncytium: an alternative to the Langendorff method. *Int J Artif Organs* 2011; **34**:546–558.
25. Burger NB, Bekker MN, de Groot CJ, Christoffels VM, Haak MC. Why increased nuchal translucency is associated with congenital heart disease: a systematic review on genetic mechanisms. *Prenat Diagn* 2015; **35**:517–528.

26. Gassmann M, Casagranda F, Orioli D, Simon H, Lai C, Klein R, Lemke G. Aberrant neural and cardiac development in mice lacking the ErbB4 neuregulin receptor. *Nature* 1995; **378**:390–394.
27. Chen H, Shi S, Acosta L, Li W, Lu J, Bao S, Chen Z, Yang Z, Schneider MD, Chien KR, Conway SJ, Yoder MC, Haneline LS, Franco D, Shou W. BMP10 is essential for maintaining cardiac growth during murine cardiogenesis. *Development* 2004; **131**: 2219–2231.
28. Watanabe Y, Zaffran S, Kuroiwa A, Higuchi H, Ogura T, Harvey RP, Kelly RG, Buckingham M. Fibroblast growth factor 10 gene regulation in the second heart field by Tbx1, Nkx2-5, and Islet1 reveals a genetic switch for down-regulation in the myocardium. *Proc Natl Acad Sci USA* 2012; **109**:18273–18280.
29. Yamada M, Revelli JP, Eichele G, Barron M, Schwartz RJ. Expression of chick Tbx-2, Tbx-3, and Tbx-5 genes during early heart development: evidence for BMP2 induction of Tbx2. *Dev Biol* 2000; **228**:95–105.
30. Kokubo H, Tomita-Miyagawa S, Hamada Y, Saga Y. Hesr1 and Hesr2 regulate atrioventricular boundary formation in the developing heart through the repression of Tbx2. *Development* 2007; **134**:747–755.
31. Yan C, Miller CL, Abe J. Regulation of phosphodiesterase 3 and inducible cAMP early repressor in the heart. *Circ Res* 2007; **100**:489–501.
32. Schott JJ, Benson DW, Basson CT, Pease W, Silberbach GM, Moak JP, Maron BJ, Seidman CE, Seidman JG. Congenital heart disease caused by mutations in the transcription factor NKX2-5. *Science* 1998; **281**:108–111.
33. Misra C, Sachan N, McNally CR, Koenig SN, Nichols HA, Guggilam A, Lucchesi PA, Pu WT, Srivastava D, Garg V. Congenital heart disease-causing Gata4 mutation displays functional deficits in vivo. *PLoS Genet* 2012; **8**:e1002690.
34. Molkentin JD, Lin Q, Duncan SA, Olson EN. Requirement of the transcription factor GATA4 for heart tube formation and ventral morphogenesis. *Genes Dev* 1997; **11**: 1061–1072.
35. Sedmera D, Harris BS, Grant E, Zhang N, Jourdan J, Kurkova D, Gourdie RG. Cardiac expression patterns of endothelin-converting enzyme (ECE): implications for conduction system development. *Dev Dyn* 2008; **237**:1746–1753.
36. Shou W, Aghdasi B, Armstrong DL, Guo Q, Bao S, Charng MJ, Mathews LM, Schneider MD, Hamilton SL, Matzuk MM. Cardiac defects and altered ryanodine receptor function in mice lacking FKBP12. *Nature* 1998; **391**:489–492.
37. Gonzalez JP, Ramachandran J, Xie LH, Contreras JE, Fraidenraich D. Selective connexin43 inhibition prevents isoproterenol-induced arrhythmias and lethality in muscular dystrophy mice. *Sci Rep* 2015; **5**:13490.
38. Darrow BJ, Laing JG, Lampe PD, Saffitz JE, Beyer EC. Expression of multiple connexins in cultured neonatal rat ventricular myocytes. *Circ Res* 1995; **76**:381–387.
39. Paulson AF, Lampe PD, Meyer RA, TenBroek E, Atkinson MM, Walseth TF, Johnson RG. Cyclic AMP and LDL trigger a rapid enhancement in gap junction assembly through a stimulation of connexin trafficking. *J Cell Sci* 2000; **113**(Pt 17): 3037–3049.
40. Salameh A, Krautblatter S, Karl S, Blanke K, Gomez DR, Dhein S, Pfeiffer D, Janousek J. The signal transduction cascade regulating the expression of the gap junction protein connexin43 by beta-adrenoceptors. *Br J Pharmacol* 2009; **158**:198–208.
41. Moorman A, Webb S, Brown NA, Lamers W, Anderson RH. Development of the heart: (1) formation of the cardiac chambers and arterial trunks. *Heart* 2003; **89**: 806–814.
42. Wessels A, Sedmera D. Developmental anatomy of the heart: a tale of mice and man. *Physiol Genomics* 2003; **15**:165–176.
43. Chen H, Zhang W, Sun X, Yoshimoto M, Chen Z, Zhu W, Liu J, Shen Y, Yong W, Li D, Zhang J, Lin Y, Li B, VanDusen NJ, Snider P, Schwartz RJ, Conway SJ, Field LJ, Yoder MC, Firulli AB, Carlesso N, Towbin JA, Shou W. Fkbp1a controls ventricular myocardium trabeculation and compaction by regulating endocardial Notch1 activity. *Development* 2013; **140**:1946–1957.
44. Jerome LA, Papaioannou VE. DiGeorge syndrome phenotype in mice mutant for the T-box gene, Tbx1. *Nat Genet* 2001; **27**:286–291.
45. Lindsay EA, Vitelli F, Su H, Morishima M, Huynh T, Pramparo T, Jurecic V, Ogunrinu G, Sutherland HF, Scambler PJ, Bradley A, Baldini A. Tbx1 haploinsufficieny in the DiGeorge syndrome region causes aortic arch defects in mice. *Nature* 2001; **410**: 97–101.
46. Rochais F, Sturny R, Chao CM, Mesbah K, Bennett M, Mohun TJ, Bellusci S, Kelly RG. FGF10 promotes regional foetal cardiomyocyte proliferation and adult cardiomyocyte cell-cycle re-entry. *Cardiovasc Res* 2014; **104**:432–442.
47. Greulich F, Rudat C, Kispert A. Mechanisms of T-box gene function in the developing heart. *Cardiovasc Res* 2011; **91**:212–222.
48. Stennard FA, Costa MW, Lai D, Biben C, Furtado MB, Solloway MJ, McCulley DJ, Leimena C, Preis JI, Dunwoodie SL, Elliott DE, Prall OW, Black BL, Fatkin D, Harvey RP. Murine T-box transcription factor Tbx20 acts as a repressor during heart development, and is essential for adult heart integrity, function and adaptation. *Development* 2005; **132**:2451–2462.
49. Harrelson Z, Kelly RG, Goldin SN, Gibson-Brown JJ, Bollag RJ, Silver LM, Papaioannou VE. Tbx2 is essential for patterning the atrioventricular canal and for morphogenesis of the outflow tract during heart development. *Development* 2004; **131**:5041–5052.
50. Barnes RM, Harris IS, Jaehnig EJ, Sauls K, Sinha T, Rojas A, Schachterle W, McCulley DJ, Norris RA, Black BL. MEF2C regulates outflow tract alignment and transcriptional control of Tdgf1. *Development* 2016; **143**:774–779.
51. Christoffels VM, Hoogaars WM, Tessari A, Clout DE, Moorman AF, Campione M. T-box transcription factor Tbx2 represses differentiation and formation of the cardiac chambers. *Dev Dyn* 2004; **229**:763–770.
52. Moskowitz IP, Kim JB, Moore ML, Wolf CM, Peterson MA, Shendure J, Nobrega MA, Yokota Y, Berul C, Izumo S, Seidman JG, Seidman CE. A molecular pathway including Id2, Tbx5, and Nkx2-5 required for cardiac conduction system development. *Cell* 2007; **129**:1365–1376.
53. Wang J, Greene SB, Bonilla-Claudio M, Tao Y, Zhang J, Bai Y, Huang Z, Black BL, Wang F, Martin JF. Bmp signaling regulates myocardial differentiation from cardiac progenitors through a MicroRNA-mediated mechanism. *Dev Cell* 2010; **19**:903–912.
54. Singh R, Horsthuis T, Farin HF, Grieskamp T, Norden J, Petry M, Wakker V, Moorman AF, Christoffels VM, Kispert A. Tbx20 interacts with smads to confine tbx2 expression to the atrioventricular canal. *Circ Res* 2009; **105**:442–452.
55. Mehel H, Emons J, Vettel C, Wittkopper K, Seppelt D, Dewenter M, Lutz S, Sossalla S, Maier LS, Lechene P, Leroy J, Lefebvre F, Varin A, Eschenhagen T, Nattel S, Dobrev D, Zimmermann WH, Nikolaev VO, Vandecasteele G, Fischmeister R, El-Armouche A. Phosphodiesterase-2 is up-regulated in human failing hearts and blunts beta-adrenergic responses in cardiomyocytes. *J Am Coll Cardiol* 2013; **62**:1596–1606.
56. Zoccarato A, Surdo NC, Aronsen JM, Fields LA, Mancuso L, Dodoni G, Stangherlin A, Livie C, Jiang H, Sin YY, Gesellchen F, Terrin A, Baillie GS, Nicklin SA, Graham D, Szabo-Fresnais N, Krall J, Vandeput F, Movsesian M, Furlan L, Corsetti V, Hamilton G, Lefkimmiatis K, Sjaastad I, Zaccolo M. Cardiac hypertrophy is inhibited by a local pool of cAMP regulated by phosphodiesterase 2. *Circ Res* 2015; **117**:707–719.
57. Baldini A. Dissecting contiguous gene defects: tBX1. *Curr Opin Genet Dev* 2005; **15**: 279–284.